

Anomalous electronic conductance in quasicrystals

Stephan Roche

* *Department of Applied Physics, University of Tokyo, 7-3-1 Hongo, Bunkyo-ku, Tokyo 113-8654, Japan.*
(February 5, 2020)

Generic quantum interference effects occurring in 1D-quasicrystals are shown and discussed in details. By defining specific geometrical defects, so-called phasons, one shows that conversely to metallic systems quantum conductance in quasiperiodic systems enclosed original behavior with respect to the alteration of its properties while downgrading long range order. This is in close conjunction with a still opened problematic in the field of quasicrystalline materials.

PACS numbers: 72.90.+y 61.44.Br 72.10.-d

I. INTRODUCTION

The understanding of exotic electronic properties of quasicrystals¹ remain quite unsatisfactory although quasicrystalline materials have already found many coating applications². In particular, the role of quasiperiodic order on electronic localization and transport is believed to entail the most unexpected experimental features whereas so far no coherent theoretical framework has been successfully established³⁻⁶. As a matter of fact, one of the most surprising features of quasicrystalline transport is the enhancement of conductive ability upon increasing contribution of static (structural defects) or dynamical excitations (phonons). This has been strongly supported by many experimental evidences³ and is often referred as the most original property in the litterature. Notwithstanding, on the theoretical side, given heuristical arguments^{4,7} and performed numerical investigations (e.g. the Landauer conductance for quasiperiodic Penrose lattices⁸ or Kubo formula for 3D-quasiperiodic models⁹) yield to uncomplete understanding of the observed properties. It is generally assumed that a specific “geometrical localization process” takes place in quasicrystals (sustained by critical states^{10,11}) and that local disruptions of corresponding mesoscopic order reduce quantum interferences, resulting in an increase of conductivity. This important statement has been unfortunately poorly considered up to now, and it is the purpose of the present work to contribute to this issue.

In what follows, exact results on 1D quasiperiodic chains will show that indeed, quasiperiodic order manifest such abovementioned amazing features. Defining a toy-defect, we will present an energy-dependent phase diagram for continuous schrodinger Kronig-Penney models. Effects of imperfections on spectrum and transport will be analyzed in details.

II. INTRODUCTION

Pioneer works of M. Kohmoto¹⁰ on multifractal properties of critical states in 1D-quasiperiodic chains have

been recently followed by renewed focus on the relation between localization features of such states and their ability to convey current¹¹. Still, variety of critical states let the question unresolved. The effect of disorder on top of these states is then a complicated issue and very scarce rigorous results are available in the litterature.

Introducing disorder could be done through typical randomizing of site or hopping energies, with the subsequent occurrence of Anderson localization in the infinite chain limit. For finite systems, localization lengthes may be much larger than the characteristic size so that conductance fluctuations as a function of energy of tunneling electrons (from the leads to the system) keep its self-similar nature and still follow power law behavior for system size studied in¹² even when introducing disorder of 10% of the total bandwith. However, the particular order sustaining long range quasiperiodicity suggest the possible presence of unique defects, known as phason-type defects. Their geometrical definition and properties have been subjected to many studies¹³, although some aspects remain controversial. From certain viewpoint it seems natural to consider how disruptions of quasiperiodic order inherent to such systems will degrade or improve transport properties. It is the aim of this work to contribute to such more general and fundamental understanding of electronic propagation in quasicrystals.

For 1D-quasiperiodic systems, we define phasons that keep the essential characteristic of real systems, in the sense that they are a generic form of disorder which has no equivalent in usual metallic and periodic systems. In a preliminary study, such phason defects were introduced, by the present author, as a main probe for investigating Landauer conductance¹⁴. The results presented here will clarify and generalized previous study.

III. TIGHT-BINDING VERSUS CONTINUOUS VERSIONS OF THE PROBLEM

Tight-binding models (TBM) of perfect quasiperiodic chains have been intensively worked out both analytically and numerically only for some given energies, but the results are supposed to have provided typical features of

localization in quasiperiodic structures, such as power-law decrease of wavefunctions or power-law bounded resistances¹⁰. However, if leading to interesting analytical results, TBM do not allow to simply investigate energy-dependent properties of quantum dynamics and electronic transport. Following the works and discussions of Kollar and Sütő¹⁵, and M. Baake et al.¹⁶, we will indeed show the limitations of TBM when compared to continuous models, for the special case of effects of phason-type disorder on electronic localization and propagation.

Tight-binding expression of the hamiltonian reads $\mathcal{H} = \sum_n t_n (|n\rangle\langle n+1| + |n+1\rangle\langle n|)$ and the projection of Schrödinger equation on a localized basis gives

$$\begin{pmatrix} \psi_{n+1} \\ \psi_n \end{pmatrix} = M_n \begin{pmatrix} \psi_n \\ \psi_{n-1} \end{pmatrix} = M_n M_{n-1} \dots M_1 \begin{pmatrix} \psi_1 \\ \psi_0 \end{pmatrix} = P_n \begin{pmatrix} \psi_1 \\ \psi_0 \end{pmatrix} \quad (1)$$

with ψ_n the component of wavefunction for energy E at site n

$$M_n = \begin{pmatrix} 0 & -\frac{t_{n-1}}{t_n} \\ 1 & 0 \end{pmatrix} \quad \text{and } P(n) = \prod_{i=1}^n M_i \quad (2)$$

Overlap integrals are given by $t_n = f(\theta_n)$ with θ_n ¹⁷ is a kind of phase and n a link index, so that $\theta_n = \frac{n}{\tau} + \theta_0(\text{mod}1)$

$$f(\theta) = t_A \quad \text{for} \quad 1/\tau^2 \leq \theta < 1$$

In what follows, the $N(i+1)$ -term of the sequence \mathcal{S} will not correspond to $N+1$ sites but to the number of allowed sites as deduced from the above-mentioned Fibonacci sequence. Fig. ?? shows a small chain with 5 sites. The construction of a phason is illustrated below for a $N=29$ site chain. Taking $\gamma = t_A/t_B$, transfer matrix can be evaluated analytically as well as the Landauer resistances. Defining the matrices $\mathcal{A}, \mathcal{B}, \mathcal{C}$ by

$$\mathcal{A} = \begin{pmatrix} 0 & -\frac{1}{\gamma} \\ \gamma & 0 \end{pmatrix} \quad \mathcal{B} = \begin{pmatrix} \gamma & 0 \\ 0 & \frac{1}{\gamma} \end{pmatrix} \quad \mathcal{C} = \mathcal{B}\mathcal{A} = \begin{pmatrix} 0 & -1 \\ 1 & 0 \end{pmatrix} \quad (3)$$

One shows that the sequence P_N follows a Fibonacci sequence. Besides, noticing that $\mathcal{CA} = \mathcal{C}$, $\mathcal{AC} = \mathcal{CA}^{-1}$ and $\mathcal{C}^2 = -\mathbb{1}$, one shows that whatever P_N there exist a recurrent structure given by $\mathcal{C}^{t(N)} \mathcal{A}^{s(N)}$

$$P_N = \begin{pmatrix} 0 & -1 \\ 1 & 0 \end{pmatrix}^{t(N)} \begin{pmatrix} \gamma & 0 \\ 0 & \frac{1}{\gamma} \end{pmatrix}^{s(N)} \quad (4)$$

where $\theta_0 = 0$ for the usual Fibonacci chain. The quasiperiodic chain corresponding to an initial phase $\theta_0 = m/\tau$ is associated with the Fibonacci sequence taken at m^{th} site of the usual one. We define the phason as a abrupt geometrical transition between the two chains with $\theta_0 = 0, 2/\tau$. The function $f(\theta_n)$ will take two values t_A or t_B , according to the link. This gives a deterministic way to construct phason defects, which break long range quasiperiodic order, but which is a kind of disorder which has no equivalent in periodic systems. Introducing a so-called local isomorphism class by changing initial phase θ_0 randomly chosen between 0 and 1, statistical studies of the localization and transport properties of Fibonacci chains have been performed^{17,18}.

A. Effect of a phason-defect at $E=0$ with TBM

In a transmission study, we define the boundary conditions as $t_N = t_0 = t_{ext} = t_B$ (Fig. ??), which lead to special values of the number of sites. From the two Fibonacci chains with $\theta = 0, 2/\tau$, the corresponding sequence is $N(i = 1, 2, 3, 4, \dots) = 4, 12, 17, 25, 33, 38, 46, 51, 59, \dots$ noticing that the difference between two consecutive numbers follow a Fibonacci sequence with numbers 8 and 5 (8,5,8,8,5,8,5,8,...).

where $t(N)$ are integers and $s(N)$ are described by a recursive relation. For the Fibonacci sequence $N = \{F_1, F_2, \dots, F_{N-1}, F_N\}$, H. Kubo and M. Goda¹⁷ have investigated the statistical properties of $s(N)$ which are directly related to the characteristical exponents of self-similar wavefunctions. Taking $(\psi_0, \psi_{-1}) = (-i, 1)$, it is possible to show that $|\psi_n|^2 = \gamma^{-2s(N) \times (-1)^{t(N)}}$. The Landauer resistance of a finite chain N is given by $\rho_N = \frac{h}{e^2} \frac{R}{T}$ where T is the fraction of tunneling electrons transmitted from the system to the leads, and R is the reflected one. For a tight-binding model one relates the resistance to the total transfer matrix elements: $\rho_N = \frac{1}{4}(P_N^2(1, 1) + P_N^2(1, 2) + P_N^2(2, 1) + P_N^2(2, 2) - 2)$. and one write the Fibonacci chain's resistance in a closed form

The function $s(N)$ is illustrated on Fig.?? which manifest self-similar pattern. When $s(N_0) = 0$, transmission is perfect $T = 1$. We now compare the effect of phason defect on the Landauer resistance. To that end, one notes that the position of the defect, represented by a -BB- unit has to be taken as an internal degree of freedom. We show that actually at $E=0$, the properties of the matrices $\mathcal{A}, \mathcal{B}, \mathcal{C}$ are independent of the position henceforth called x_P . By simple manipulations of the transfer matrix, we further demonstrate that the total transfer matrix associated to the chain with one phason and with $N(i)$ links is the same as the one without phason but with $N(i+2)$ links. Accordingly, a generic form can be written down : P_N (with either $a = d = 0$, or $b = c = 0$)

$$P_{N(i)}|_I = \begin{pmatrix} a & b \\ c & d \end{pmatrix} \quad (5)$$

then

$$P_{N(i)}|_{III} = P_{N(i+2)}|_I = - \begin{pmatrix} 0 & -\gamma \\ 1 & 0 \end{pmatrix} \begin{pmatrix} 0 & -\frac{1}{\gamma} \\ 1 & 0 \end{pmatrix} \begin{pmatrix} a & b \\ c & d \end{pmatrix} \quad (6)$$

Landauer resistance is thus given by :

$$(\rho_N)_{III} = \left(\frac{\gamma^{s(N)-1} - \gamma^{-s(N)+1}}{2} \right)^2$$

By comparing the two expressions for the Landauer resistance one concludes that at $E = 0$, the sign of $\rho_N|_I - \rho_N|_{III}$ is fluctuating as a function of chain-length, which means the phason defect does not alter the transport properties in the infinite limit.

To conclude let us consider Lyapunov exponent for finite length systems since they are interestingly related to estimates of the associated localization lengthes at a given energy¹⁹. By definition effective Lyapunov exponents (since localization length can be much larger than system size in the finite limit) for a chain of N sites are given by $\rho_N(E) = \frac{h}{2e^2} \exp(\gamma_N(E) \times N)$ which is equivalent to $\gamma_N(E) = \frac{1}{N} |P_N(1,2)|^2$ (given that $\rho_N(E) = |P_N(1,2)|^2$).

In our case, energies lying outside the spectrum are easily identified with stronger Lyapunov exponent as exemplified on Fig.???. The cantor spectrum for eigenvalues is revealed by the corresponding self-similar pattern of localization lengthes distribution. More detailed analysis of the consequence of phason disorder on lyapunov exponents is underway.

B. High density of phason-defects

We now consider the sequence constructed following the same algorithm but maximizing the number of phason defects as identified by **BB**. We then calculated analytically the Landauer resistance $\rho_N|_{IV}$. For instance for chains with $N=4$ and $N=17$ links, one has :

$$(B) - ABBA - (B)$$

$$(B) - ABBABBAABABBABAA - (B)$$

With the same transfer matrices previously introduced \mathcal{A}, \mathcal{B} and noticing that BAABAB and BAB are equal respectively to \mathcal{A} and $-\mathcal{B} = \tilde{\mathcal{B}}$, we show that the sequence of $P_N|_{IV}$ is generated by the following Fibonacci sequence $P_N = \mathcal{A}, \mathcal{A}\tilde{\mathcal{B}}, \mathcal{A}\tilde{\mathcal{B}}\mathcal{A}, \mathcal{A}\tilde{\mathcal{B}}\mathcal{A}\mathcal{A}\tilde{\mathcal{B}}, \mathcal{A}\tilde{\mathcal{B}}\mathcal{A}\mathcal{A}\tilde{\mathcal{B}}\mathcal{A}\tilde{\mathcal{B}}\mathcal{A}, \mathcal{A}\tilde{\mathcal{B}}\mathcal{A}\mathcal{A}\tilde{\mathcal{B}}\mathcal{A}\mathcal{A}\tilde{\mathcal{B}}\mathcal{A}\mathcal{A}\tilde{\mathcal{B}}, \dots$. The analytical form of $\rho_N|_{IV}$ is shown to be given by

$$(\rho_N)_{IV} = \left(\frac{\gamma^{\tilde{s}(N)} - \gamma^{-\tilde{s}(N)}}{2} \right)^2$$

with $\tilde{s}(N)$ a new complex function of N calculated iteratively. The interesting point to observe is that the function $\rho_N|_I - \rho_N|_{III}$ for one phason defect changes its sign at each step $N \rightarrow N + 1$, whereas $\rho_N|_I - \rho_N|_{IV}$ manifestes fluctuations on much larger range. As an illustration, chains with number of sites respectively equal to $N(i = 1, 2, 3, 4, 5 \dots 17) = 5 - 203$ sites follow $\rho_N|_I - \rho_N|_{IV} \geq 0$, whereas the behavior is opposite for chain from 330 to 456 sites, and so forth.

In conclusion, even for the highest density, such phason disruptions of quasiperiodic order are not able to break down the localization mechanism which do remain basically the same in the limit $N \rightarrow \infty$.

IV. LANDAUER RESISTANCE OF A KRÖNIG PENNEY MODEL WITH PHASON

In this model, the potenial describing the interaction of the electron with the lattice is represented by a sum of Dirac distributions with intensity V_n localized at x_n ²⁰

$$V(x) = \sum_n V_n \delta(x - x_n)$$

the x_n, V_n can be chosen as correlated variables, or uncorrelated. In between two successive scattering centers, the solution of the Schrödinger equation is a linear combination of two plane waves:

$$\Psi(x) = A_n e^{ik(x-x_n)} + B_n e^{-ik(x-x_n)} \quad (x_n \leq x \leq x_{n+1})$$

the 1D wavevector $k > 0$ is related to the energy E through $E = \hbar^2 k^2 / 2m$. In the Krönig-Penney (KP)²⁰ model, a solution of the problem is constructed by imposing continuity conditions for the wavefunction and its derivative. For sake of simplicity, we choose the case where the intensity of scattering potential is constant $= \lambda$

, whereas scattering centers are quasiperiodically spaced $\{(x_n - x_{n-1})\} = \{a, b\} = \{\tau, 1\}$. The problem can then be written as followed :

$$\begin{pmatrix} A_{n+1} \\ B_{n+1} \end{pmatrix} = \Lambda(n) \cdot \begin{pmatrix} A_n \\ B_n \end{pmatrix} \quad (7)$$

with

$$\Lambda(n) = \begin{pmatrix} (1 - \frac{i\lambda}{2k})e^{ik(x_{n+1}-x_n)} & -\frac{i\lambda}{2k}e^{ik(x_{n+1}-x_n)} \\ \frac{i\lambda}{2k}e^{-ik(x_{n+1}-x_n)} & (1 + \frac{i\lambda}{2k})e^{-ik(x_{n+1}-x_n)} \end{pmatrix} \quad (8)$$

The resistance can be written down analytically at k_s

$$\rho_N|_{k=k_s} = \left(\frac{\lambda}{2k_s} \right)^2 \frac{\sin^2 N\varphi}{\sin^2 \varphi} \quad (10)$$

with φ , depending on k_s^2 and λ , and is defined equivalently by $\cos \varphi = \cos k_s a + \lambda/2k_s \sin k_s a$ or $\cos \varphi = \cos k_s b + \lambda/2k_s \sin k_s b$. The analytical form of $\rho_N|_{k=k_s}$ indicates that when $N \rightarrow \infty$, the Landauer resistance oscillates but remains bounded, so that the energies k_s^2 corre-

within this framework, Landauer resistance is given by $\rho_N = |P_n(1, 2)|^2$ with $P_n = \Lambda(F_n) \dots \Lambda(1)$. Furthermore, a renormalization group associated with the Fibonacci chain enables to map the electronic spectrum to a dynamical system associated with the traces of the transfer matrices. The following energy-dependent invariant of the Krönig-Penney model is convenient to consider²¹. In our case, we find $I(k) = \frac{\lambda^2 \sin^2 k(a-b)}{4k^2}$ whose zeros are given by $k_s = n\pi/(a-b)$, with n integer. These points referred as conducting points are interesting since they correspond to the commutation of the transfer matrices, $[P_{F_n}, P_{F_{n+1}}] = 0$ given that $4I + 2 = \text{Tr}(P_{F_n} \cdot P_{F_{n+1}} \cdot P_{F_n}^{-1} \cdot P_{F_{n+1}}^{-1})$. Besides elementary matrices also commute :

$$[\Lambda(\Delta x = a), \Lambda(\Delta x = b)] = \lambda \frac{e^{ik(a-b)}}{4k^2} (1 - e^{2ik(b-a)}) \begin{pmatrix} \lambda & \lambda - 2ik \\ -\lambda - 2ik & -\lambda \end{pmatrix} \quad (9)$$

spond to states that lead to best transmission, reminding that localized states will display exponential increase of resistance. Following the discussion of^{15,16}, we will now restrict the study for energies $k^2 = (k_s + \varepsilon)^2$ in the vicinity of k_s where highest density of eigenvalues are expected in the infinite limit. The results presented henceforth will be limited to the vicinity of $k_s = \pi/(\tau-1)$, ($a = \tau, b = 1$) without loss of generality. Two transfer matrices are then defined

$$\Lambda_A = \begin{pmatrix} (1 - \frac{i\lambda}{2k})e^{ik\tau} & -\frac{i\lambda}{2k}e^{ik\tau} \\ \frac{i\lambda}{2k}e^{-ik\tau} & (1 + \frac{i\lambda}{2k})e^{-ik\tau} \end{pmatrix} \quad \Lambda_B = \begin{pmatrix} (1 - \frac{i\lambda}{2k})e^{ik} & -\frac{i\lambda}{2k}e^{ik} \\ \frac{i\lambda}{2k}e^{-ik} & (1 + \frac{i\lambda}{2k})e^{-ik} \end{pmatrix} \quad (11)$$

We choose λ so that $\rho_N|_{k=k_s} = 0$ exactly at $k = k_s$, which lead to $N-1$ values for λ , given by $\lambda_s = \frac{2k_s(\cos \varphi_s - \cos k_s)}{\sin k_s}$ with the phase φ_s defined through $\varphi_s = (m\pi)/N$ with $m=1, \dots, N-1$. The $N-1$ values φ_s are symmetrically distributed around $\pi/2$ and cover densely the half-upper trigonometric plane when increasing N . Detailed analysis of the energy-dependant phase diagram of $\rho_N(x_P, \varphi_s, \varepsilon)$ is summarized afterwards. The main definitions to understand the diagram and the corresponding patterns are :

- x_P : the position of phason defect (**BB**) in the chain, with $x_P \in [1, P]$ an integer P the maximum number of position for a given chain
- $\varphi_s = m\pi/N$, $m = 1, \dots, N-1$: the phase of the scattering potential λ with $\lambda < 0$ for a potential well and $\lambda > 0$ for the barrier case.
- ε , and $k^2 = (k_s + \varepsilon)^2$ the energy of the incident tunneling electrons k_s ($k_s = \pi/(\tau-1)$)

Numerical accuracy is checked through $P_N(1, 1)^2 - 1 = P_N(1, 2)^2$ which gives the resolution. The Landauer resistance calculated in $k = k_s$ is always found to be $\sim 10^{-12} - 10^{-13}$ and gives thus the numerical uncertainty on ρ_N . We now present the main results as sketched on the phase diagram in Fig.???. According to the variable φ_s ones identifies several features. First, note that amazing pseudo-symmetry is found around $\pi/2$ for $\rho_N(x_P, m, \varepsilon)$ which do not correspond to any symmetry in the scattering potential (see below Fig.??-?? for illustration).

In the zones referred as zone-**I** the phason is shown to systematically reduce the resistance for energies sufficiently close to the conducting points (see Fig.??-??). We will come with the energy issue later on. Two symmetric zones are $m < N - 4P$, and $m > 4P$ with $\rho_N|_{I}(x_P, m, \varepsilon) > \rho_N|_{III}(x_P, m, \varepsilon)$. In other words, for that values of parameters the Fibonacci chain becomes more conductive upon introduction of local phason. This

effect is a pure result of quantum interference at low temperature and has been shown for tunneling energies close to the ones of conducting points, so for the electrons that can better contribute to conduction mechanism. We

FIBO : -- *B* -- *ABAABABAABABAABABAABAABABAABABAAB* -- *B* --
Def1 : -- *B* -- **AB***BABAABAABABAABABAABAABAABAB* -- *B* --
Def2 : -- *B* -- *ABAABABBAABABAABAABAABAABAABAB* -- *B* --
Def3 : -- *B* -- *ABAABABAABBABAABABAABAABAABAABAB* -- *B* --
Def4 : -- *B* -- *ABAABABAABAABABBABAABAABAABAABAABAB* -- *B* --
Def5 : -- *B* -- *ABAABABAABAABAABABAABBABAABAABAABAABAB* -- *B* --
Def6 : -- *B* -- *ABAABABAABAABAABAABAABBABAABAABAABAABAB* -- *B* --
Def7 : -- *B* -- *ABAABABAABAABAABAABAABAABAABAABAABBBABAABAB* -- *B* --
Def8 : -- *B* -- *ABAABABAABAABAABAABAABAABAABAABAABAABBABAABAB* -- *B* --

Besides, the function $\rho_N|_{\text{III}}(k, m, x_P)$ given a kind of interference pattern described by the position of phason defect $\rho_N|_{\text{III}}(k, m, x_P) \sim \alpha(m/P) \sin(\frac{2m\pi}{P}x_P)$. This is further represented on Fig.?? for chains with $N=2000$ links, and $m=1.5$. The curves for $m=1$ (Fig.?? and Fig.??(top)) and different chain lengths shows that the interference pattern encloses a memory of self-similarity.

The power spectrum of $m=5$ curve is given on Fig.??, where the only eigenfrequency agrees with $m/P = 5/472 = 0.0106$ in this case. Superimposed small oscillations are an unphysical effect due to a Fourier transform

$$\Lambda_A = \begin{pmatrix} (1 - \frac{i\lambda}{2k})e^{ik\tau} & -\frac{i\lambda}{2k}e^{ik\tau} \\ \frac{i\lambda}{2k}e^{-ik\tau} & (1 + \frac{i\lambda}{2k})e^{-ik\tau} \end{pmatrix}$$

A first order development, in $\varepsilon = k - k_s$, of the Landauer resistance $\rho_N = |P_N(1, 1)|^2 - 1 = |P_N(1, 2)|^2$ yields

$$\rho_4|_{\text{I}} = 45.3087 \left(k - \frac{\pi}{\tau - 1} \right)^2 + \dots \quad (13)$$

$$\rho_4|_{\text{III}} = 30.7868 \left(k - \frac{\pi}{\tau - 1} \right)^2 + \dots \quad (14)$$

which gives a systematic increasing of conductance upon introduction of defect, whatever the energy. For larger chains, analytical calculations become more cumbersome, and one has to recourse numerical computation.

Let's move forward to zone-**II**. for $N - 4P < m < 4P$ situations becomes more complex but recurrent simple $(m - P)$ -periodic oscillatory patterns are found around the values $\varphi_s = \{(N - 4P)/N, (N - 3P)/N, (N - 2P)/N, (N - P)/N\} \pi$ and symmetrically for $\tilde{\varphi}_s =$

illustrate these behaviors first on Fig.?? which allow to write down all the 8 different inequivalent defected-chains as described below for clarity for a system with 35 sites:

of a finite signal.

The existence of a finite energy range around $k = k_s$ satisfying such pattern can be analytically illustrated on the smallest chain and $n = 1$ ($k_s = \frac{\pi}{\tau - 1}$), $m = 1$ ($\varphi_s = \pi/5$), represented by

I : ...*BBBBB(B)ABAAB(B)BBBBB*...

III : ...*BBBBBB(B)ABBABA(B)BBBBB*...

the two total transfer matrices are $P_4|_{\text{I}} = \Lambda_B \Lambda_A \Lambda_A \Lambda_B \Lambda_A$ and $P_4|_{\text{III}} = \Lambda_B \Lambda_A \Lambda_B \Lambda_B \Lambda_A$ with

$$\Lambda_B = \begin{pmatrix} (1 - \frac{i\lambda}{2k})e^{ik} & -\frac{i\lambda}{2k}e^{ik} \\ \frac{i\lambda}{2k}e^{-ik} & (1 + \frac{i\lambda}{2k})e^{-ik} \end{pmatrix} \quad (12)$$

$\{4P/N, 3P/N, 2P/N, P/N\}\pi$. In these regions of parameter space, there is an genuine transition from systematic increasing to decreasing (and vice versa) of the electronic resistance upon introduction of phason, as exemplified on Fig.??.

As far as zone-**III** is concerned, and related to some interval around $\varphi \sim \frac{\pi}{2}$, self similar patterns are observed which suggest that $\rho_N|_{\text{III}}(x_P)$ reveal critical states which are robust against phason disorder as found in the TBM for $E=0$ case. The typical patterns represented on Fig.?? actually encloses oscillations of resistance which smaller oscillations are described by some coefficients $s(n)$ as described previously.

On the Fig.??, the case with 3000 sites is considered and different values of the scattering potential in the vicinity of the symmetry point $\varphi = \frac{\pi}{2}$. For $m=1497$, the potential is $\lambda \sim 3.918$, for $m=1498$ $\lambda \sim 3.929$ and 3.941 for $m=1499$. Patterns exhibit small differences, and their Fourier spectrum is actually very similar (see below).

The power spectra of different similar patterns are given on Fig.?? and Fig.?? which show that superimposed frequencies are identical. The highest frequency is given by $\nu = 0.5$ which is related to the change of $\rho_N(x_P \rightarrow x_P + 1)$. On respective figures five unambiguous frequencies have been located and named $\nu_{n=1,5}$. This prove that all these self-similar patterns are actually described by exactly the same function which is a superposition of several independent frequencies convolute with a function defined by a serie of $s(N)$ -type coefficients. Concerning all the discussed zones-**I**, **II**, **III**, one has found surprising simple forms for energies sufficiently close to conducting points. Then $\rho_N(x_P, \varepsilon)$ are more or less simple superposition of one or several frequencies. For larger energies one finds fluctuations as those analyzed in the inset of Fig.?. As energies get farther to conducting points $k_s = \pi/(\tau - 1)$ the resistance is sharply increasing on several order of magnitudes. The power spectrum in this case reveal much more eigenfrequencies, with the interesting emergence of frequencies with similar amplitudes refered as ν and ω . In all these cases the respective behaviors of the Landauer resistance of the perfect Fibonacci chain versus the imperfect one follows complicated random fluctuations.

The different behaviors found in these studies suggest that in some case local disruption of long range quasiperiodic order has improved the conductive ability of the chain in a systematic manner. Analyzing the interference pattern of the Landauer resistance as a function of phason defect suggest that extendedness (as a localization properties of available states at such energies) has also been jointly improved. This is shown by a bounded and simple oscillatory pattern for the resistance, common to what is found for extended eigenstates in a periodic systems.

To conclude this study, one stresses that first conducting points indeed seem to be the location of high density of eigenenergies as discussed in^{15,16}, and with the help of Krönig Penney model we have been able to unravel specific quantum interference effects of phason disorder on localization and propagation properties, hidden in the treatment of TBM, and appealing in the context of quasicrystalline materials.

V. CONCLUSION

Several features occurring in the electronic transport of quasicrystals in 1D have been presented. Quantum interferences have been shown to be interestingly altered by phason defects which may be a natural disruption of quasicrystalline disorder. In the energy range where the highest concentration of conducting points is expected, phason defects were shown to upgrade Landauer conductance under certain circumstances.

ACKNOWLEDGMENTS

S.R. is indebted to the European Commission for financial support (Contract ERBIC17CT980059), and to Prof. T. Fujiwara from Department of Applied Physics of Tokyo University for his warm hospitality. Udo Beierlein, Kostas Moulopoulos, and Gabriel Roche are acknowledged for encouragements.

¹ D. Shechtman, I. Blech, D. Gratias et J.W. Cahn, *Phys. Rev. Lett.* **51**, 1951 (1984).

² J.M. Dubois et al. *Annales de Chimie* **19**, 3 (1994). S. Roche, *Annales de Chimie* **23**, 953 (1998). E. Maciá, in *Revista Española de Física* (may 1998).

³ C. Berger, *Seminar 3*, E. Akkermans, G. Montambaux, J.L. Pichard and J. Zinn-Justin eds. *Les Houches, Session LXI, Mesoscopic Quantum Physics* (1994).

⁴ S. Roche, G. Trambly de Laissardière and D. Mayou, *J. of Math. Phys.* **38**, 1794 (1997).

⁵ T. Fujiwara, in *Physical Properties of Quasicrystals*, Springer Series in Solid-State Sciences **126**, Editor Z.M. Stadnik, 169 (1999)

⁶ S. Roche and T. Fujiwara, *Phys. Rev. B* **58**, 11338 (1998).

⁷ C. Sire in "Lectures on Quasicrystals", ed. F. Hippert and D. Gratias (Les Editions de Physique Les Ulis, 1994).

⁸ S. Yamamoto and T. Fujiwara, *Phys. Rev. B* **51**, 8841 (1995).

⁹ S. Roche and D. Mayou, *Phys. Rev. Lett.* **79**, 2518 (1997).

¹⁰ M. Kohmoto, L. P. Kadanoff, and Ch. Tang, *Phys. Rev. Lett.* **50** 1870 (1983); *ibid.* **50** 1873 (1983). M. Kohmoto, *Intern. J. of Mod. Phys. B* **1** 31 (1986). M. Kohmoto and J. R. Banavar, *Phys. Rev. B* **34** 563 (1986).

¹¹ E. Maciá and F. Domínguez-Adame, *Phys. Rev. Lett.* **76**, 2957 (1996). and references therein.

¹² S. Das Sarma and X.C. Xie, *Phys. Rev. B* **37**, 1097 (1988).

¹³ T.C. Lubensky, J.E.S. Socolar, P.J. Steinhardt, P.A. Bancel and P.A. Heiney, *Phys. Rev. Lett.* **57**, 1440 (1986). G. Coddens, R. Bellissent, Y. Calvayrac, J.P. Ambroise, *Europhys. Lett.* **16** 271 (1991). A. Trub and H.R. Trebin, *J. Phys. France* **4** 1855-1866 (1994). H. Klein, M. Audier, M. Boudarda and M. de Boissieu, L. Behara and D. Duneau, *Phil. Magazine A* **73**, 309-331 (1996).

¹⁴ K. Moulopoulos and S. Roche, *Phys. Rev. B* **53**, 212 (1996).

¹⁵ J. Kollar and A. Süto, *Physics Letters A* **117**, 203 (1986).

¹⁶ M. Baake, D. Joseph and P. Kramer, *Phys. Lett. A* **168**, 203 (1986).

¹⁷ M. Goda and H. Kubo, *J. Phys. Soc. Jpn.* **58** 3624 (1989) ; H. Kubo and M. Goda, *J. Phys. Soc. Jpn.* **60** 2729 (1991) ; *J. Phys. Soc. Jpn.* **62** 2601 (1993).

¹⁸ F. Wijnands, *J. Phys. A* **22**, 3267 (1989).

¹⁹ A. Süto, in *Beyond quasicrystals*, edited by F. Axel and D. Gratias (Les Editions de Physique, France, 1994) 483.

²⁰ R. de L. Krönig and W.G. Penney, in *Mathematical Physics in One Dimension*, eds. E.H. Lieb and D.C. Mattis, p. 243.

²¹ M. Baake, U. Grimm and D. Joseph, Int. Journ. of Moder. Phys. B, **7** Nos. 6&7 (1993) 1527.

Figure captions

Fig1 Chain $N = 4$: ABAA connected with perfect leads.

Fig2 Multifractal distribution of $|s(N)|$ for the Fibonacci chain of 800 sites.

Fig3 Lyapunov exponents as a function of energy of a Fibonacci chain.

Fig4 Energy dependent phase diagram.

Fig5 Landauer resistance as a function of phason position x_P , for $\varepsilon = 10^{-4}$, $N = 35$ sites and $m=1$.

Fig6 Landauer resistances as a function of phason position x_P ($N=2001, P=472$) for $\varepsilon = [10^{-9}, 10^{-6}]$ and $m=5$. For higher values of ε , then $\rho_N \rightarrow \infty$ which indicates that energy lies within a gap, or may be associated with a localized state.

Fig7 Power spectrum of the pattern given in the inset for $m=5$ and same parameters as previous figure (bottom).

Fig8 Regular evolution of interference pattern for $m = P, P+1, P+2$ and $N = 2000, P = 472$. For $\varphi_s = P\pi/N$, Fibonacci chain is always less resistive than the imperfect one whereas transition occurs for $m = P + 1, P + 2, \dots$ dashed curves are the values for Fibonacci chains with same parameter m as imperfect one.

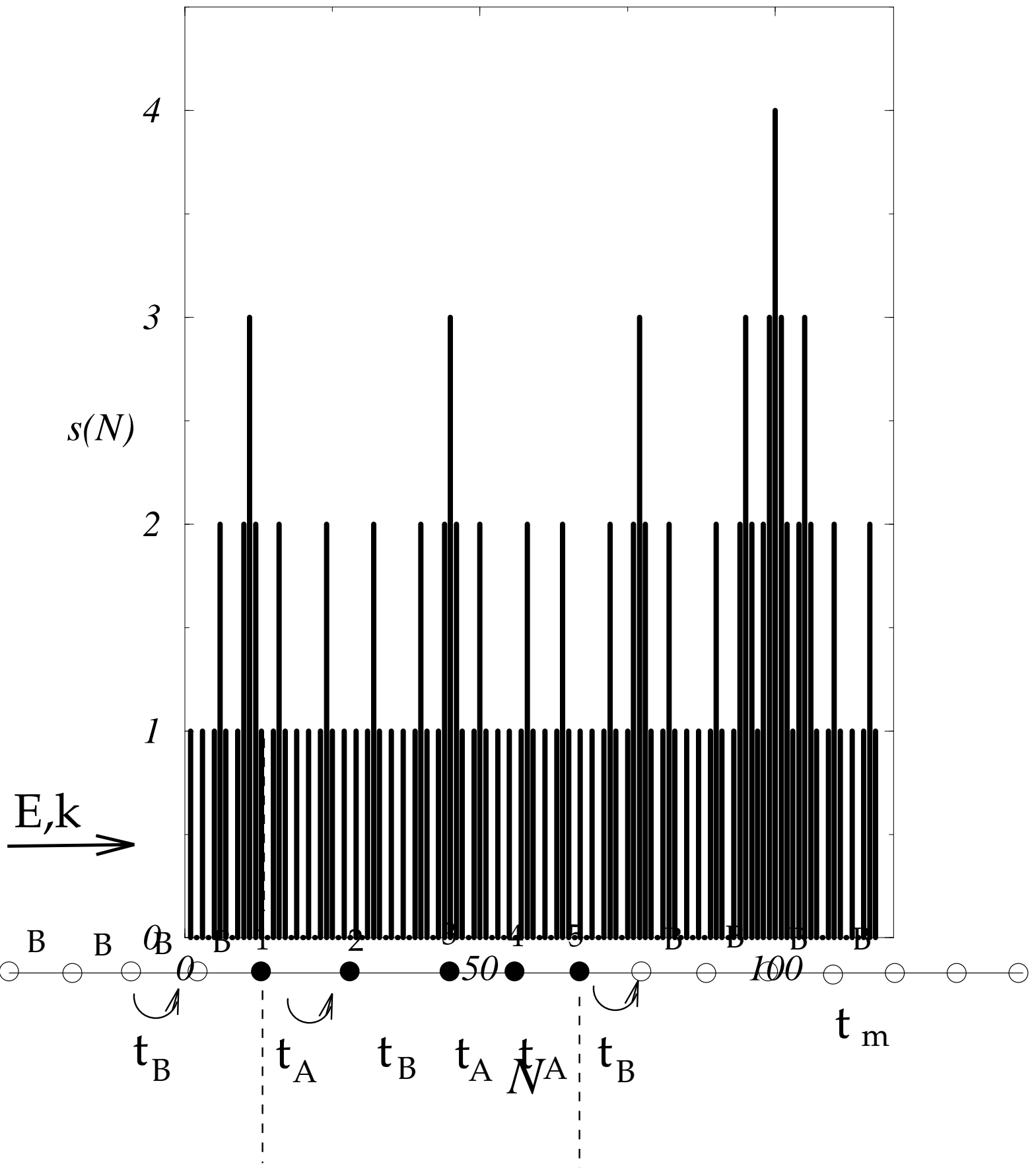
Fig9 Landauer resistance for values of scattering potential which unravel self-similar patterns as described in the text.

Fig10 Interference pattern for several values of scattering potentials close to $\varphi \sim \frac{\pi}{2}$.

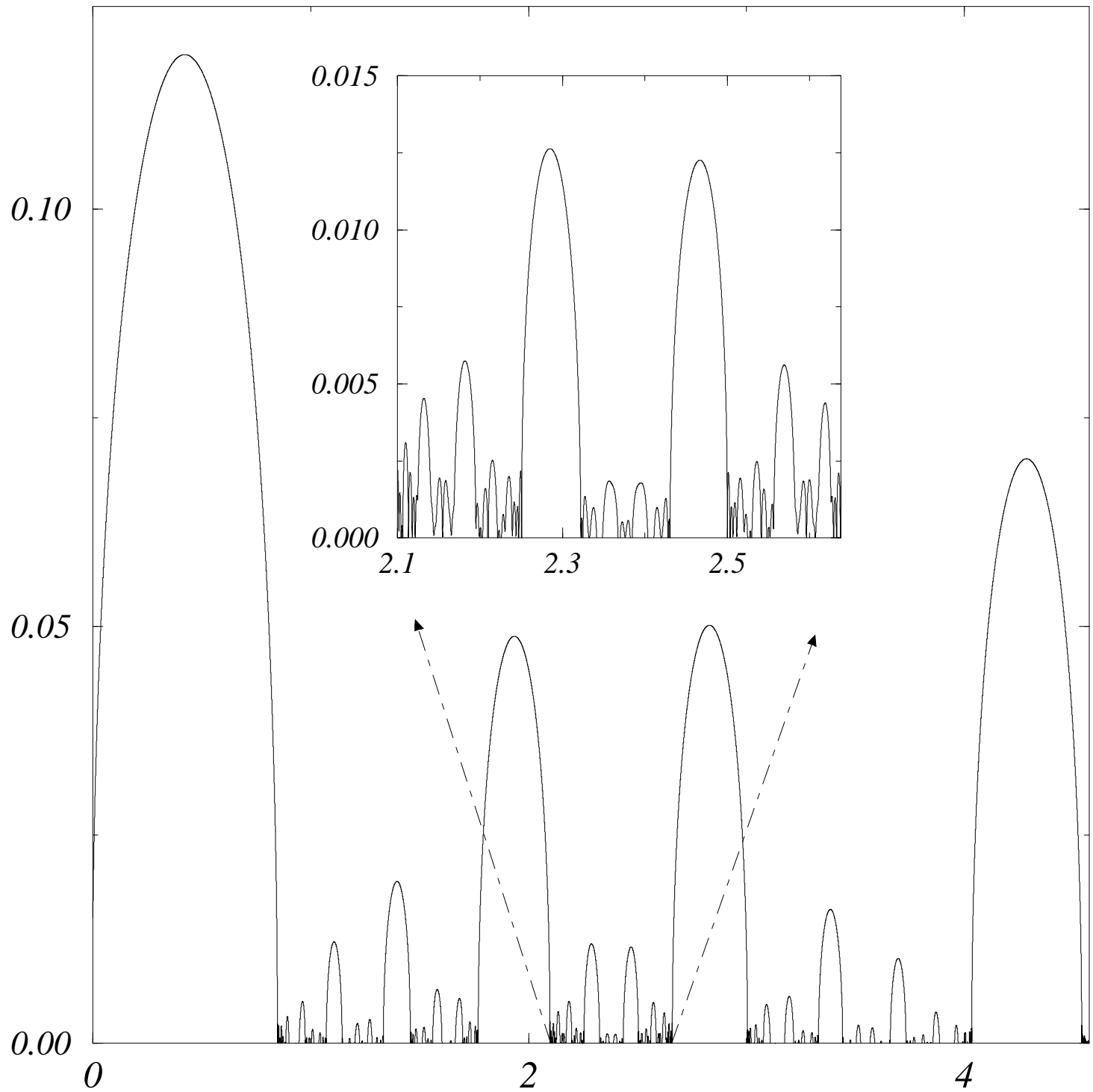
Fig11 Self similar interference pattern for $N=3207$, $P=757$ and $m=1605$. Stability is ensured from $\varepsilon = 10^{-3}$ down to the numerical resolution limit.

Fig12 Same as previous figure with different m .

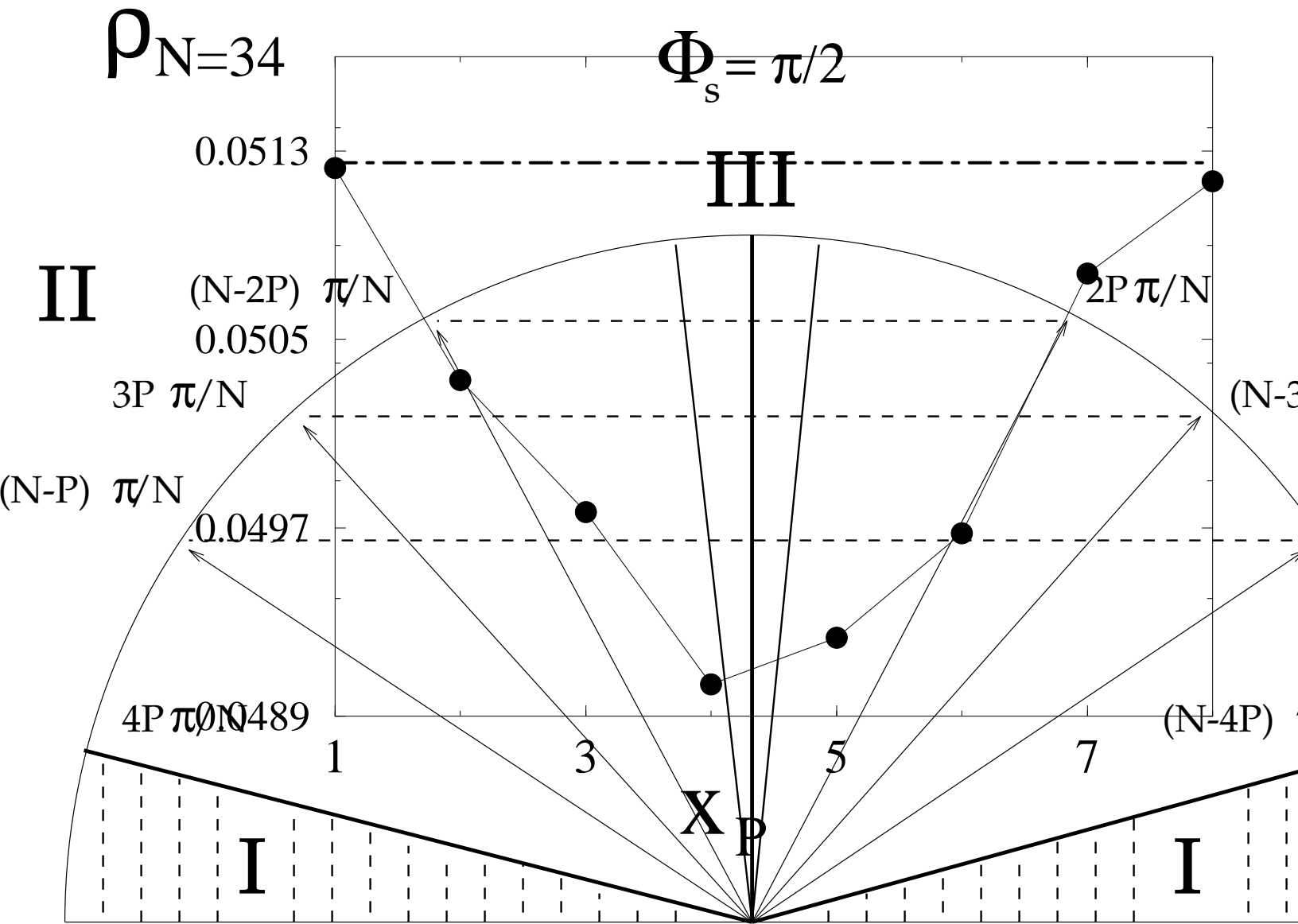
Fig13. Landauer resistance interference pattern for $\varepsilon = 0.5$, $N=2000$ and $P=472$.

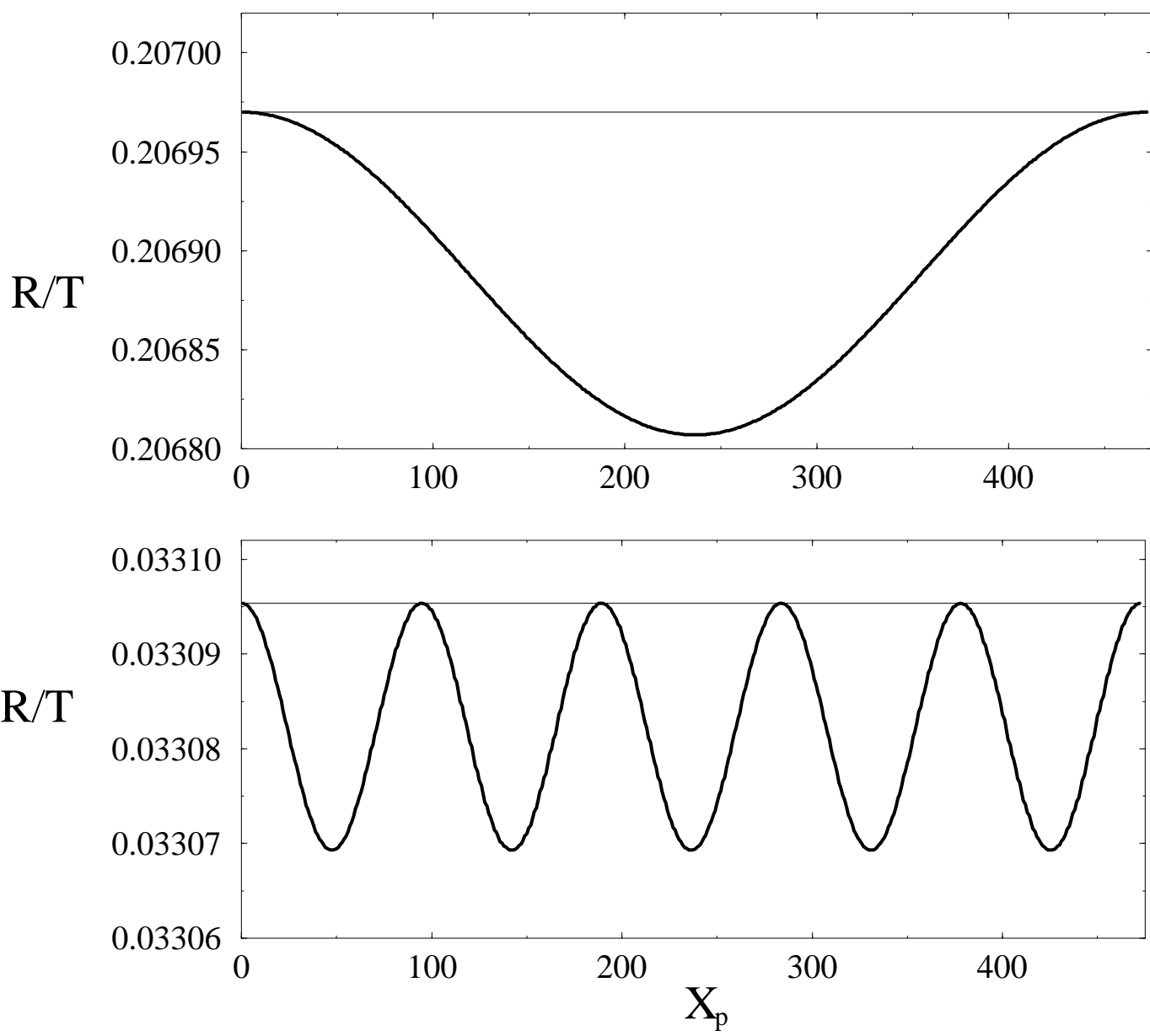


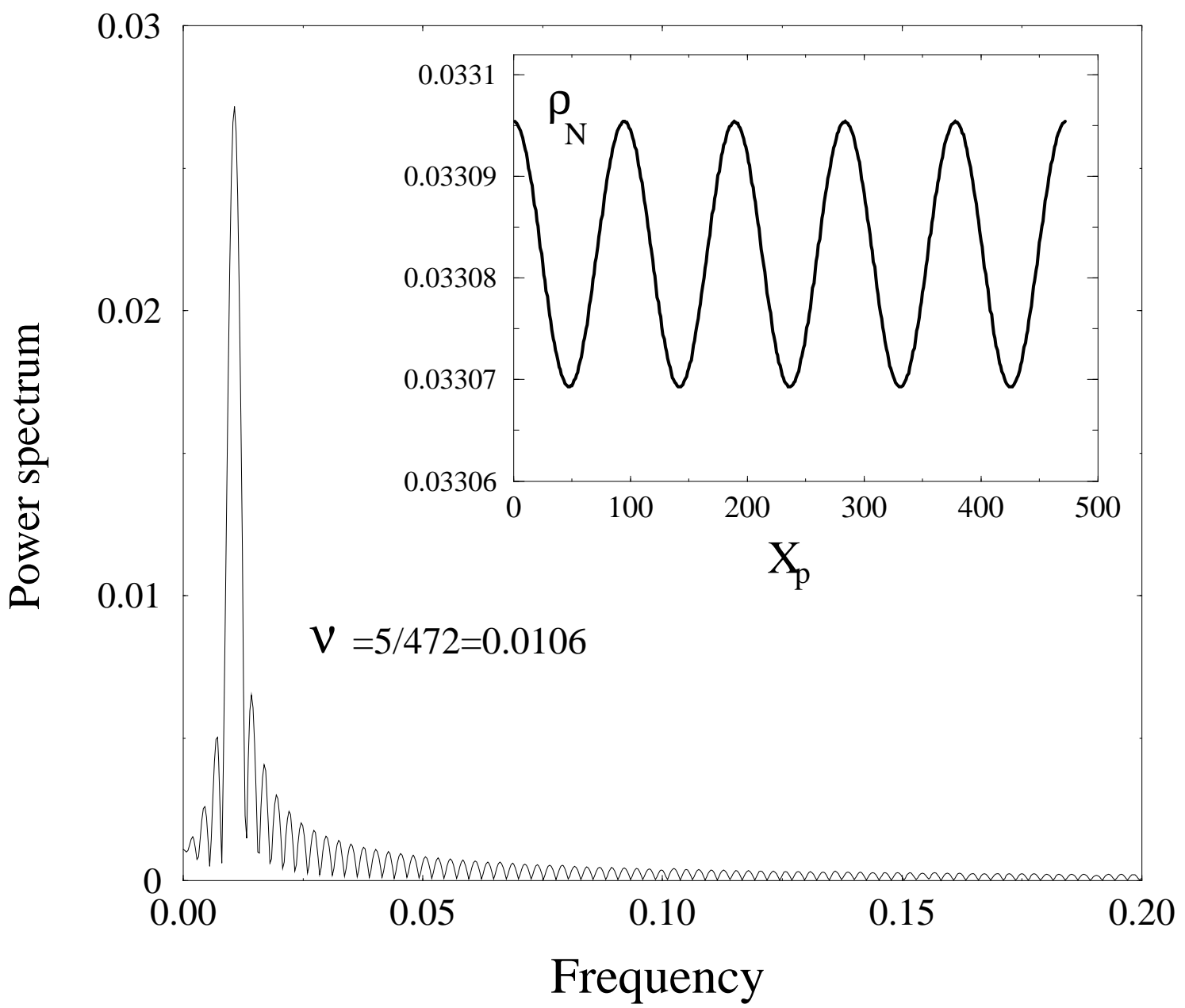
Exposant de Lyapunov γ (E)

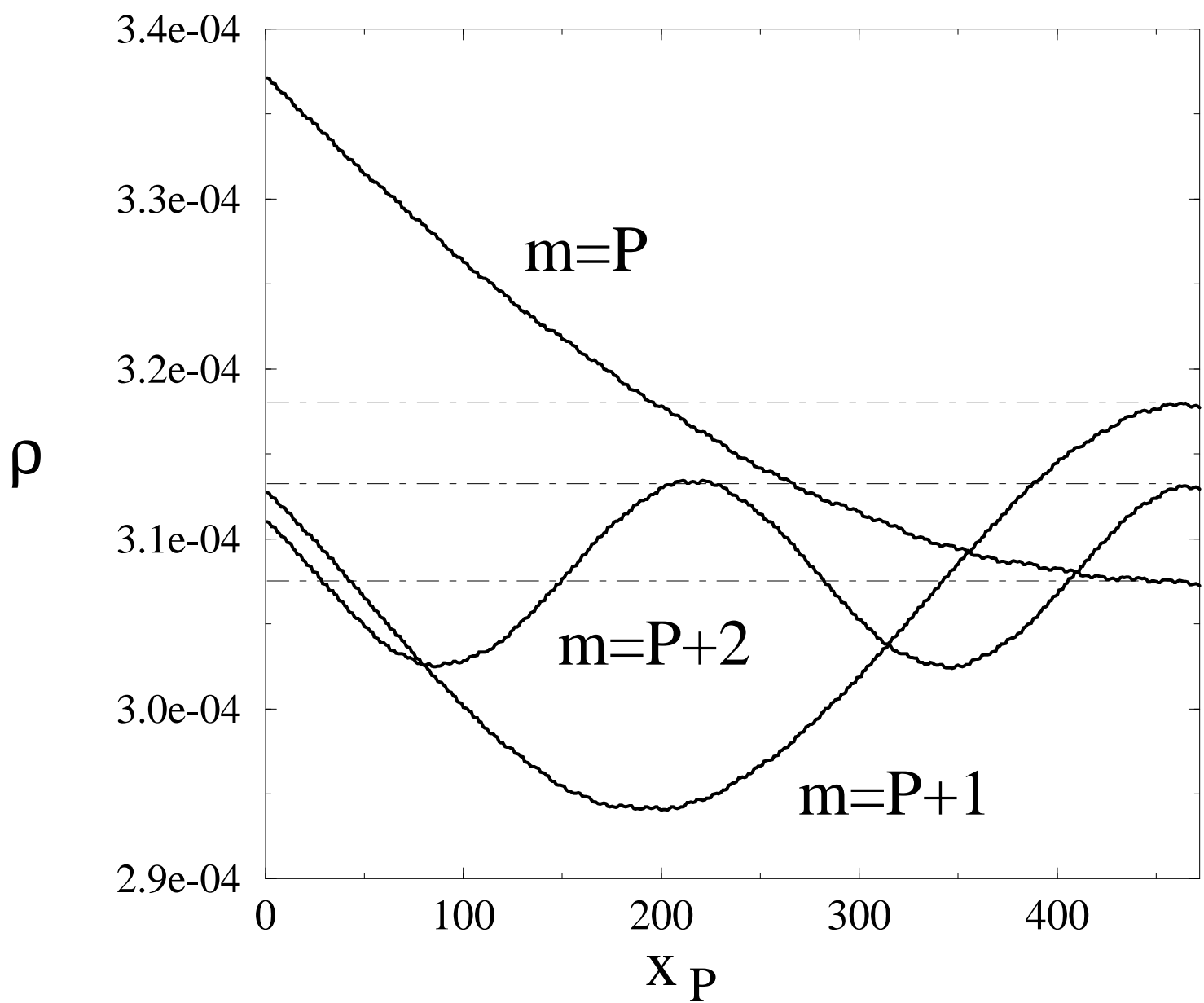


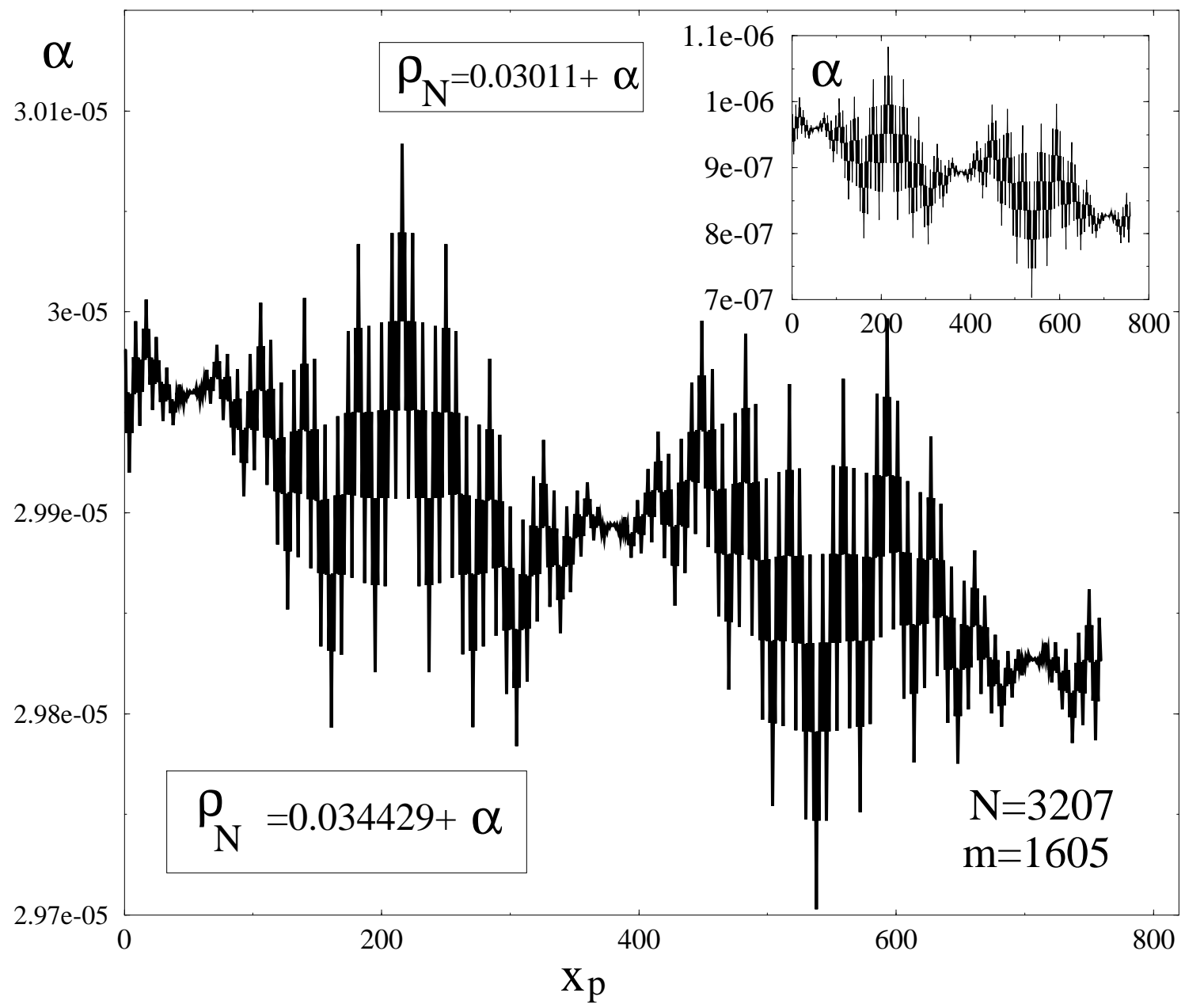
Energy

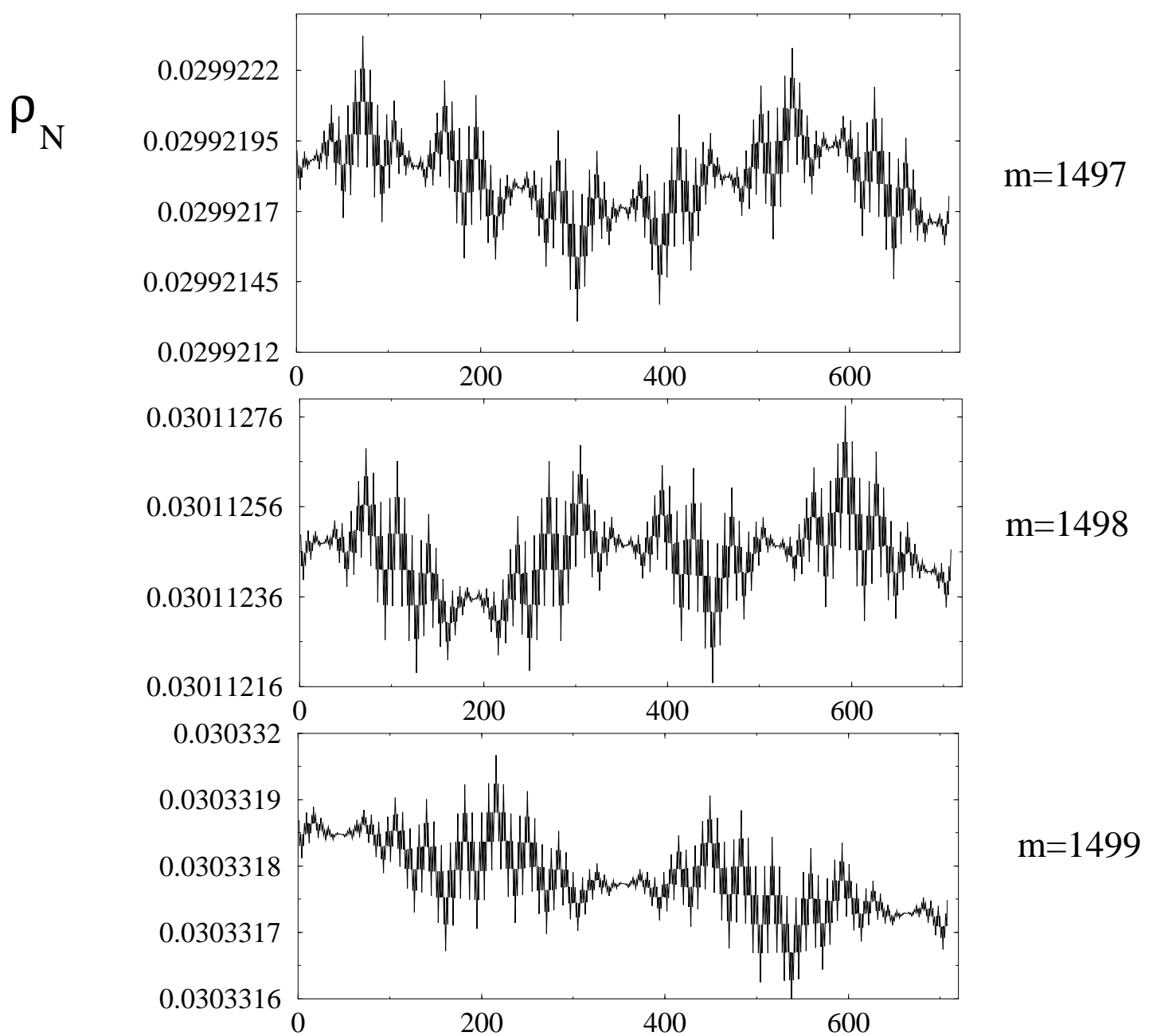


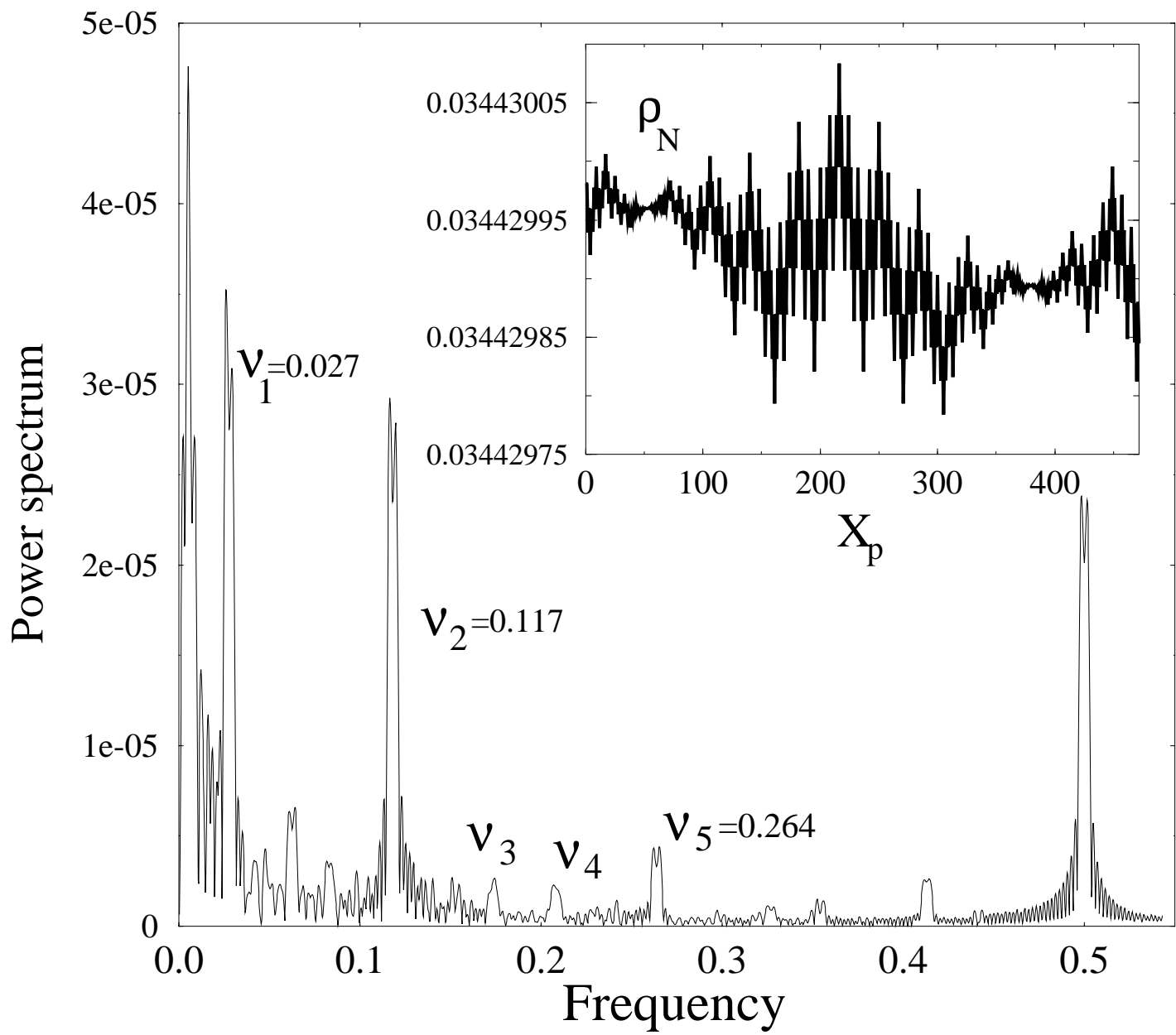


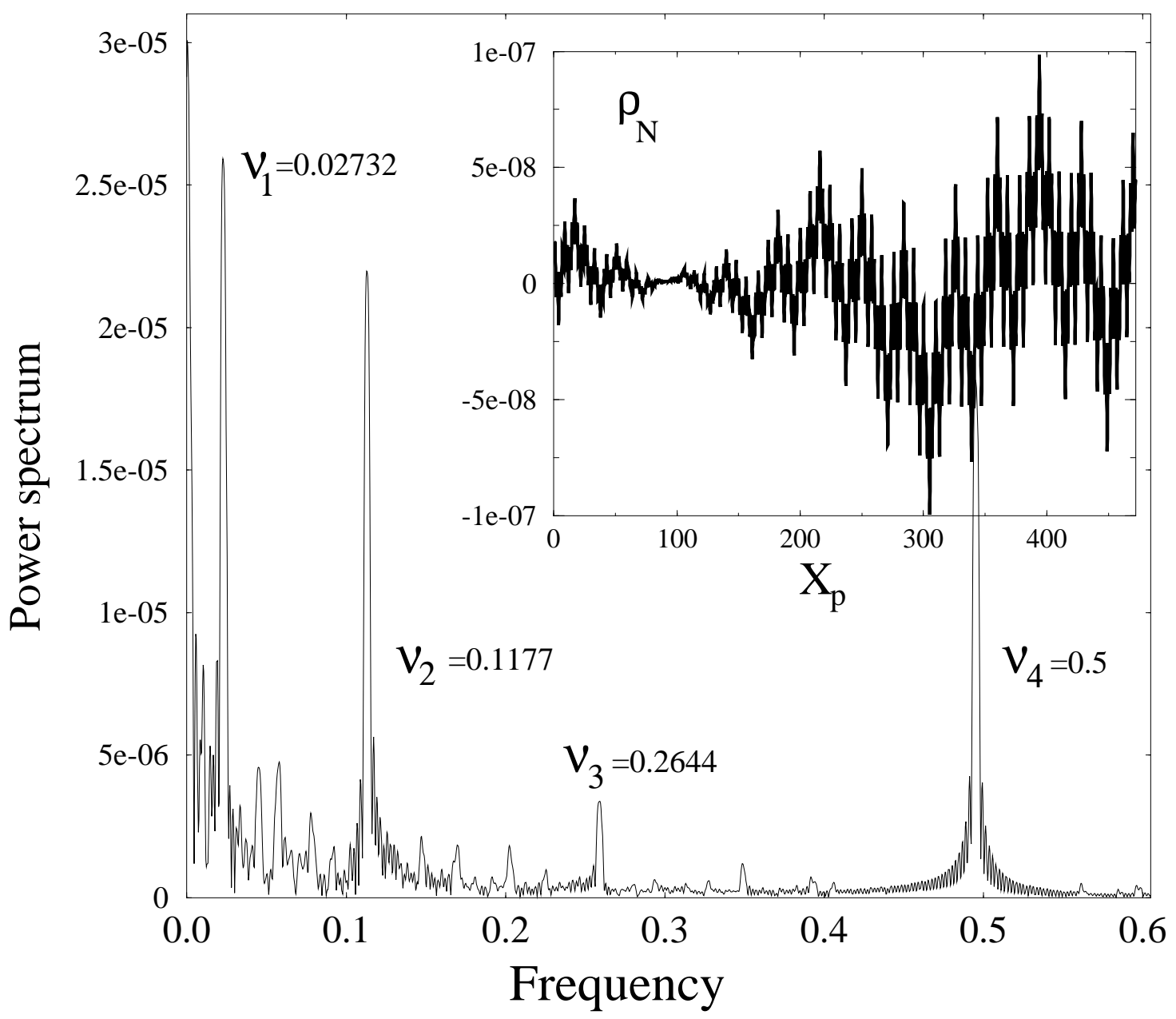












Power spectrum

